Coupling strength effect on shot noise in boron devices*

Li Gui-Qin(李桂琴)† and Guo Yong(郭 永)

Department of Physics, Tsinghua University, Beijing 100084, *China*

(Received 18 March 2013; revised manuscript received 22 April 2013)

The shot noise properties in boron devices are investigated with a tight-binding model and the non-equilibrium Green's function. It is found that the shot noise and Fano factors can be tuned by changing the structures, the size, and the coupling strength. The shot noise is suppressed momentarily as we switch on the bias voltage, and the electron correlation is significant. The Fano factors are more sensitive to the ribbon width than to the ribbon length in the full coupling context. In the weak-coupling context, the Fano factors are almost invariant with the increase of length and width over a wide bias range.

Keywords: shot noise, boron devices, coupling strength

PACS: 73.23.–b, 85.35.–p **DOI:** 10.1088/1674-1056/22/11/117304

1. Introduction

Nanoscale electronic devices have been attracting much attention,[1–8] the nanoscale systems may help minimize computer circuit dimensions and enhance the computer performance. To design electronic devices with specific properties, a basic understanding of the transport properties in the devices is necessary. The transport properties in such devices are characterized by several important factors, including the quantization of energy levels, the quantum interference of electron waves, the electronic structure of the molecule, the molecular coupling with the side attached electrodes,[8] etc. The transport properties of the electronic devices are also controlled by the carrier number, thus the shot noise is the primary noise source of interest. The noise is connected with current fluctuation.[9] There are two types of noise in the electronic devices. One is the thermal noise and the other is the shot noise. The thermal noise is a fluctuation in the occupation numbers of the states in a system caused by thermal agitation. The shot noise, current fluctuation, is a consequence of the quantization of charge and can be used to obtain some information about a system which is not directly available through conductance measurements. The noise power of current fluctuation provides additional important information about the electron correlation by calculating the Fano factor F. The Fano factor is the ratio of the actual shot noise to the Poisson noise.[9] Full shot noise is characterized by $F = 1$. With shot noise suppression, $F < 1$; and $F > 1$ for shot noise enhancement. The shot noise suppression receives a lot of attention in connection with modern electronic devices.

In this paper, we investigate the shot noise based on the tight-binding model through boron devices. Graphene, as a promising new material for electronic devices, is of considerable interest due to its peculiar electronic properties.[10–15] Many devices based on graphene ribbons have been investigated both experimentally and theoretically.[16–20] However, studies on boron revealed that the high hardness and high melting point of boron are vital to the production of electronic devices.[21–25] Researchers have proposed several boron sheet structures, such as the hexagonal graphitic boron sheet,[26] the buckled triangular boron sheet,[27] and the hybrid hexagon–triangle boron sheet.[28,29] However, the stability of the boron sheet is still an open question. The hybrid hexagon–triangle boron sheet was thought to be the most stable structure.[28,29] The density of states and transmission coefficients in a boron device have been studied.[30,31] In this paper, we investigate the effects of shot noise, Fano factor, and coupling strength on the shot noise in boron devices.

The rest of this paper is organized as follows. In Section 2, the theoretical calculation method of shot noise through a boron ribbon sandwiched between two gold electrodes is described. In Section 3, the shot noise as a function of the applied bias voltage is studied for different boron devices, and the effects of several factors on the shot noise are investigated. In Section 4, some conclusions are drawn from our investigations.

2. Theoretical calculation method

In this section, we briefly describe the calculation of shot noise in a boron device. According to the scattering theory of thermal and shot noise, the noise power of current fluctuation in the device is[9]

$$S = \frac{e^2}{\pi\hbar}\int_{-\infty}^{+\infty} \mathrm{d}E\{T[f_{\mathrm{L}}(1-f_{\mathrm{L}})+f_{\mathrm{R}}(1-f_{\mathrm{R}})] + T(1-T)(f_{\mathrm{L}}-f_{\mathrm{R}})^2\}, \quad (1)$$

*Project supported by the National Basic Research Program of China (Grants Nos. 2011CB921602 and 2011CB606405) and the National Natural Science Foundation of China (Grant Nos. 91221205 and 11174168).

†Corresponding author. E-mail: ligqin@mail.tsinghua.edu.cn

© 2013 Chinese Physical Society and IOP Publishing Ltd

where $f_{L,R} = f(E - \mu_{L,R})$ are the Fermi functions with electrochemical potentials μ_L and μ_R ($\mu_{L,R} = E_F \pm eV/2$), and T is the transmission coefficient of the system and given as $T = \mathrm{Tr}(\Gamma_1 G \Gamma_2 G^+)$, with $G(G^+)$ being the retarded (advanced) Green function, Γ describing the coupling between electrode and extend boron ribbon and being simply given by the imaginary part of the electrode self-energy. The first term on the right-hand side of Eq. (1) is the thermal equilibrium noise contribution to the noise power spectrum, and the second term is the shot noise contribution. We only consider the shot noise in this paper. We can see from Eq. (1) that the shot noise is not simply determined by the conductance of the system. Instead, it is determined by a sum of products of transmission and reflection probabilities. The Fano factor is[9]

$$F = \frac{\int_{-\infty}^{\infty} \mathrm{d}ET(1-T)(f_L - f_R)^2}{\int_{-\infty}^{\infty} \mathrm{d}ET(f_L - f_R)}. \quad (2)$$

A typical device that exhibits full shot noise ($F = 1$) is a vacuum diode operating under current saturation conditions (i.e., the noise is produced due to single independent electrons). Phenomena of shot noise suppression ($F < 1$) and enhancement ($F > 1$) can also occur in certain devices. The mechanisms for shot noise suppression or enhancement may be long-range and short-range Coulomb interactions,[32–37] elastic and inelastic scatterings, Fermi–Dirac statistics due to the Pauli principle,[9,38,39] etc.

3. Results and discussion

In this section, we investigate the shot noise in a boron device with an *ab initio* method combining with the nonequilibrium Green function technique.[40,41] The tight-binding Hamiltonian is used in the calculations. The hexagonal graphitic boron device, buckled triangular boron device, and hybrid hexagon–triangle boron device are designed as follows. The zigzag edge of the boron ribbon is contacted through a single sulfur atom to finite gold electrodes, as shown in Figs. 1(a)–1(c). The electrodes are oriented along the (111) direction and are described by clusters with three layers (three, seven, and three). The vertical distance between the S atom and the most external plane of the Au electrodes is 1.90 Å with an S–Au bond length of 2.53 Å. The other bond lengths are Au–Au 2.885 Å, S–B 1.97 Å, and B–B 1.67 Å. The structure parameters of the hexagonal graphitic boron, buckled triangular boron, and hybrid hexagon–triangle boron are based on Refs. [26]– [29].

In Fig. 2, we plot the shot noise as a function of the applied bias voltage for three different structure boron devices, where the dashed curve (curve 1) denotes the result of the hexagonal graphitic boron device, the dotted curve (curve 2) represents the result of the hybrid hexagon–triangle boron device, and the dash dotted curve (curve 3) corresponds to the result of the buckled triangular boron device. It is found from Fig. 2 that there are significant differences among the three values of shot noise. The shot noise can be greatly modulated not only by the bias voltage, but also by the structure. Curves 1 and 3 monotonically increase as the bias increases. The value of shot noise in the hybrid hexagon–triangle boron device increases with increasing bias up to 0.6 V, then it saturates at a value around 7.5×10^{-25} A^2/Hz. This means that the shot noise remains at the same level above the bias of 0.6 V.

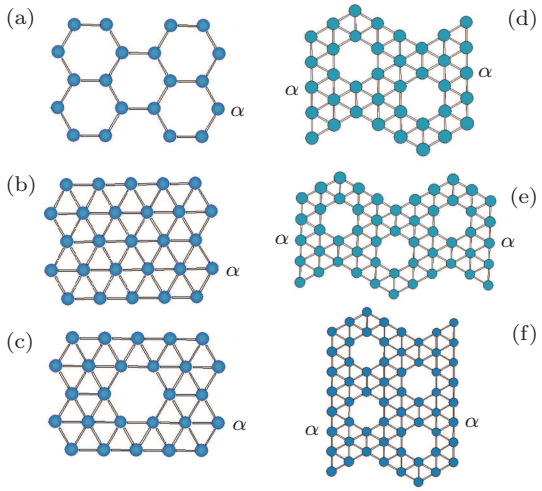


Fig. 1. (color online) Geometries of six boron ribbons, where the boron atom denoted by α is contacted through a S atom to gold electrodes: (a) hexagonal graphitic boron ribbon, (b) buckled triangular boron ribbon, (c) hybrid hexagon–triangle boron ribbon, (d) hybrid hexagon–triangle boron ribbon with 38 boron atoms, (e) hybrid hexagon–triangle boron ribbon with 52 boron atoms, and (f) hybrid hexagon–triangle boron ribbon with 60 boron atoms.

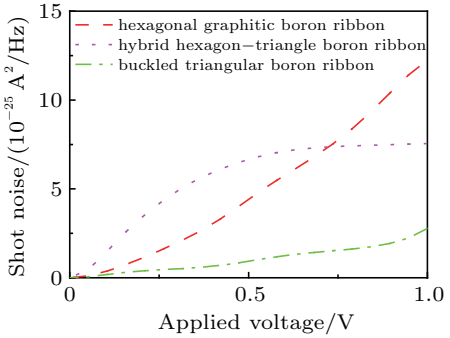


Fig. 2. (color online) Shot noise in three different boron structure devices.

To better understand the shot noise in these boron devices, we calculate their Fano factors. The details of the Fano factor versus the applied voltage are shown in Fig. 3. The Fano factors are between 0 and 1. This feature means that for these three boron devices, the shot noise is suppressed momentarily when we switch on the bias voltage and the electron correlation is very significant. Here the electron correlation only means that one electron feels the existence of the other due to the Pauli principle,[8] because we have neglected all other electron–electron interactions in our calculations. The Fano factor in the buckled triangular

boron device (curve 3) increases at some bias voltages and decreases at other bias voltages in the whole bias range investigated. It is evident that the Fano factor demonstrates a valley between 0.2 V and 0.6 V. A similar feature appeared in other research work dealing with the shot noise in the double-barrier heterostructures and the spin-dependent shot noise in diluted-magnetic-semiconductor/semiconductor heterostructures.[42,43] The Fano factor in the hexagonal graphitic boron device is almost the same as that in the hybrid hexagon–triangle boron device at the bias up to 0.5 V. At a bias higher than 0.5 V, the Fano factor in the hexagonal graphitic boron device decreases with increasing bias, however that in the hybrid hexagon–triangle boron device increases slowly with increasing bias and then is almost saturated at a value around 0.7. These features demonstrate that the electron transport capabilities are suppressed in different manners for the three devices as the applied voltage increases. The shot noise in the buckled triangular boron device is slightly suppressed compared with the other devices.

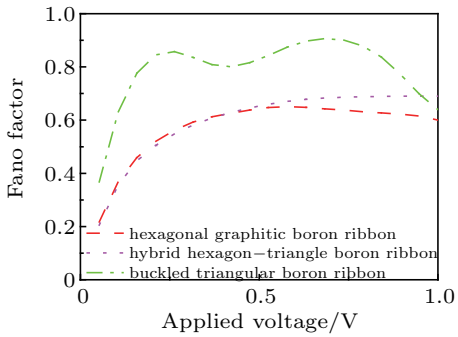


Fig. 3. (color online) Fano factor versus applied voltage for three different structure boron devices.

To demonstrate the influence of the size effect on the shot noise, we present the shot noise and Fano factors of three different-size hybrid hexagon–triangle boron devices in Figs. 4 and 5, respectively, where the solid curve corresponds to the result of the device with 38 B atoms, the dashed curve denotes the result of the device with 52 B atoms, and the dotted curve represents the result of the device with 60 B atoms. The structures of the boron ribbons are shown in Figs. 1(d)–1(f). The armchair edge of the boron ribbon is contacted through a single sulfur atom to finite gold electrodes. It is found from Fig. 4 that the shot noise shows a size-dependent behavior. As the length of the ribbon increases (corresponding to the B atoms increasing from 38 to 52), the shot noise decreases as the bias voltage decreases from 0.75 V, while slightly increases as the bias voltage increases from 0.75 V. As the width of the ribbon increases (corresponding to the B atoms increasing from 38 to 60), the shot noise decreases slightly with bias increasing up to 0.25 V, then increases excellently above 0.25 V and becomes saturated at a value around 10×10^{-25} A^2/Hz.

It is shown in Fig. 5 that the shot noise is suppressed in these three different-size devices and the electron correlation is significant. The important feature to note is that the Fano factors are all small at $V \to 0$ and each exhibit a strong increase with bias increasing up to 0.2 V. The Fano factor is almost invariant over a wide bias range as the length of the ribbon increases. However, the Fano factor decreases obviously as the width of the ribbon increases. This feature means that the electron correlation in the device with a wider boron ribbon is much more significant than that in other devices. The shot noise in the wider device is drastically suppressed over most of the bias range compared with that in other devices.

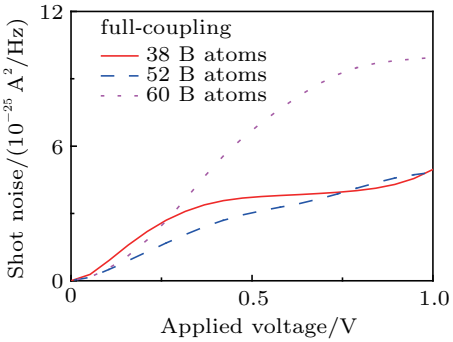


Fig. 4. (color online) Shot noise versus applied voltage in three different size hybrid hexagon–triangle boron devices at full-coupling context.

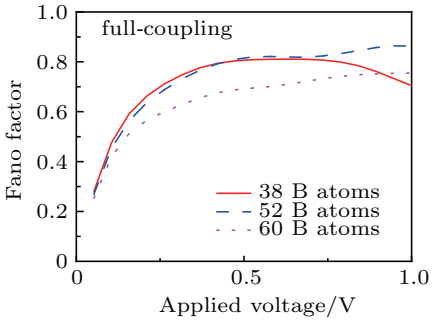


Fig. 5. (color online) Fano factor versus applied voltage in three different size hybrid hexagon–triangle boron devices at full-coupling context.

Finally, we study the shot noise in the weak-coupling devices. We reduce the self-energies of both contacts by a constant 0.5. The details of the shot noise and Fano factor in weak-coupling boron devices are shown in Figs. 6 and 7, respectively. Compared with the result in Fig. 4, the shot noise in Fig. 6 shows a strong dependence on the coupling strength. The shot noise decreases with decreasing coupling strength. This is due to the change of the energy level broadening. The contribution to the change of the energy level broadening comes from the imaginary parts of the two self-energies.[43] The Fano factor is almost invariant over a wide bias range not only as the length of the ribbon increases, but also as the width of the ribbon augments.

Figure 8 presents the densities of states (DOS) in three boron devices with different coupling strengths. The solid

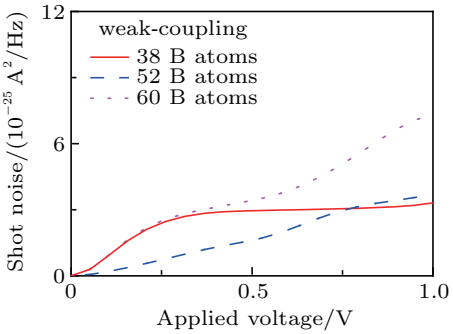


Fig. 6. (color online) Shot noise versus applied voltage in three different-size hybrid hexagon–triangle boron devices at weak-coupling context.

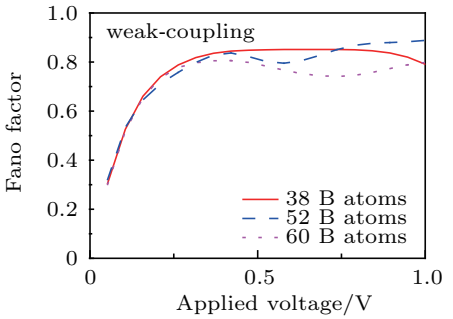


Fig. 7. (color online) Fano factor versus applied voltage in three different-size hybrid hexagon–triangle boron devices at weak-coupling context.

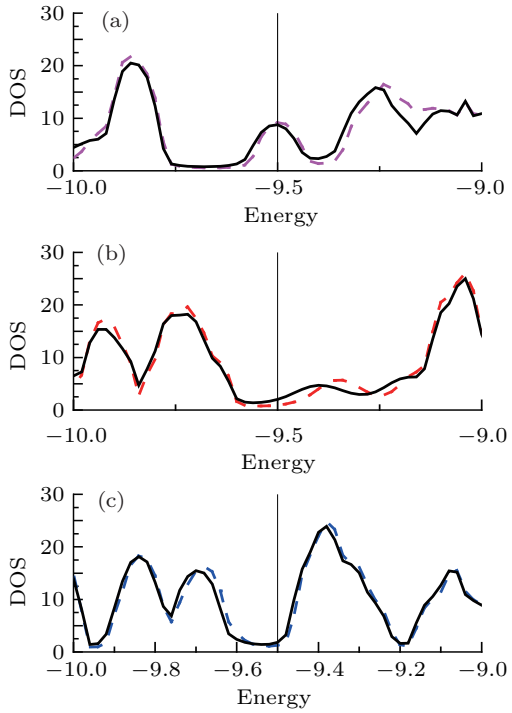


Fig. 8. (color online) (color online) Densities of states in three different-size hybrid hexagon–triangle boron devices with different coupling strengths: (a) 38 B atoms, (b) 52 B atoms, (c) 60 B atoms.

curve denotes the DOS in the full-coupling context, and the dashed curve refers to the result of the weak-coupling context. We can see that the difference in DOS for different coupling strengths near the Fermi level is not obvious. This means that the electron transmission is not obviously affected by the coupling strength. The results in Figs. 4 and 6 demonstrate that the nonequilibrium fluctuation in current measured by the shot noise is generally more sensitive to the coupling strength due to the effects of incidence and reflection, which may shed light on the subtle mechanisms in mesoscopic transport processes.

4. Conclusion

In this paper, the characteristics of shot noise in the boron devices with different structures are investigated with an *ab initio* method combining with the non-equilibrium Green's function technique. It is found that the shot noise in the boron device is greatly modulated by the applied voltage, structure of the boron, size of the boron, and coupling strength. For all devices, the shot noise is suppressed momentarily as we switch on the bias voltage and the electron correlation is very significant. The shot noise in the hybrid hexagon–triangle boron device remains at the same level above the bias of 0.6 V. The shot noise in the buckled triangular boron device is slightly suppressed compared with that in other two devices. The Fano factor in the buckled triangular boron device demonstrates a valley between 0.2 V and 0.6 V. The Fano factor in the hexagonal graphitic boron device and that in the hybrid hexagon–triangle boron device are almost the same below 0.5 V. The Fano factor in the boron device is more sensitive to the width of the ribbon than to the length of the ribbon in the full-coupling context. In the weak-coupling context, the Fano factor is almost invariant over a wide bias range as the size increases. Our results may provide ideas for fabricating efficient electronic devices.

References

[1] Yazdani A, Eigler D and Lang N 1996 *Science* **272** 1921
[2] Datta S, Tian W, Hong S, Reifenberger R, Henderson J and Kubiak C P 1997 *Phys. Rev. Lett.* **79** 2530
[3] Tian W, Datta S, Hong S, Reifenberger R, Henderson J and Kubiak C P 1998 *J. Chem. Phys.* **109** 2874
[4] Nitzan A and Ratner M A 2003 *Science* **300** 1384
[5] Zhu Z W, Hao Y, Zhang J F, Fang J P and Liu H X 2006 *Acta Phys. Sin.* **55** 5878 (in Chinese)
[6] Baadji N and Sanvito S 2012 *Phys. Rev. Lett.* **108** 217201
[7] Carrascal D, Garcia-Suarez V M and Ferrer J 2012 *Phys. Rev. B* **85** 195434
[8] Li Z L,Wang C K, Luo Y and Xue Q K 2005 *Chin. Phys.* **14** 1036
[9] Blanter Ya M and Büttiker M 2000 *Phys. Rep.* **336** 1
[10] Novoselov K S, Geim A K, Morozov S V, Jiang D, Katsnelson M I, Grigorieva I V, Dubonos S V and Firsov A A 2005 *Nature* **438** 197
[11] Zhang Y, Tan Y W, Stormer H L and Kim P 2005 *Nature* **438** 201
[12] Soodchomshom B, Tang I M and Hoonsawat R 2009 *Physica E* **41** 1310
[13] Peres N M R, Guinea F and Castro Neto A H 2006 *Phys. Rev. B* **73** 125411
[14] Nomura K and MacDonald A H 2007 *Phys. Rev. Lett.* **98** 076602
[15] Li Z Y, Qian H Y, Wu J, Gu B L and Duan W H 2008 *Phys. Rev. Lett.* **100** 206802
[16] Andriotis A N, Richter E and Menon M 2007 *Appl. Phys. Lett.* **91** 152105

[17] Koskinen P 2011 *Appl. Phys. Lett.* **99** 013105
[18] Li G Q, Ca J, Deng J K, Rocha A R and Sanvito S 2008 *Appl. Phys. Lett.* **92** 163104
[19] Soudi A, Aivazian G, Shi S F, Xu X D and Gu Y 2012 *Appl. Phys. Lett.* **100** 033115
[20] Kumar S B and Guo J 2012 *Nanoscale* **4** 982
[21] Lipscomb W L 1963 *Boron Hydrides* (New York: Benjamin W A)
[22] Meutterties E L 1974 *Boron Hydride Chemistry* (New York: Academic)
[23] Cotton F A, Wilkinson G, Murillo C A and Bochmann M 1999 *Advanced Inorganic Chemistry* (New York: Wiley)
[24] Jemmis E D, Balakrishnarajan M M and Pancharatna P D 2002 *Chem. Rev.* **102** 93
[25] Wang X J, Tian J F, Bao L H, Yang T Z, Hui C, Liu F, Shen C M, Xu N S and Gao H J 2008 *Chin. Phys. B* **17** 3827
[26] Evans M H, Joannopoulos J D and Pantelides S T 2005 *Phys. Rev. B* **72** 045434
[27] Lau K C and Pandey R 2007 *J. Phys. Chem. C* **111** 2906
[28] Tang H and Ismail-Beigi S 2007 *Phys. Rev. Lett.* **99** 115501
[29] Yang X, Ding Y and Ni J 2008 *Phys. Rev. B* **77** 041402
[30] Li G Q 2009 *Appl. Phys. Lett.* **94** 193116
[31] Li G Q 2010 *Chin. Phys. B* **19** 017201
[32] Ziel A van der 1954 *Noise* (New York: Prentice-Hall)
[33] Iannaccone G, Lombardi G, Macucci M and Pellegrini B 1998 *Phys. Rev. Lett.* **80** 1054
[34] Gonzalez T, Gonzalez C, Mateos J, Pardo D, Bulashenko O M, Ruby J M and Reggiani L 1998 *Phys. Rev. Lett.* **80** 2901
[35] Nagaev K 1998 *Phys. Rev. B* **57** 4628
[36] Kozub V and Rudin A 1995 *Phys. Rev. B* **52** 7853
[37] Hung K and Wu G 1993 *Phys. Rev. B* **48** 14687
[38] Sukhorukov E and Loss D 1998 *Phys. Rev. Lett.* **80** 4959
[39] Martin T and Landauer R 1992 *Phys. Rev. B* **45** 1742
[40] Zahid F, Paulsson M and Datta S 2003 *Advanced Semi-conductors and Organic Nanotechniques* (New York: Academic Press)
[41] Paulsson M, Zahid F and Datta S 2005 *Huckel-IV on the nanoHub*, https://www.nanohub.org/resources/422/
[42] Aleshkin V Y, Reggiani L and Rosini M 2006 *Phys. Rev. B* **73** 165320
[43] Guo Y, Han L, Zhu R and Xu W 2008 *Eur. Phys. J. B* **62** 45